Transmitted properties of terahertz wave through metallic hole arrays

Dong Li (李 栋)[1], Shiwei Shu (舒时伟)[1], Fangfang Li (栗芳芳)[1], Guohong Ma (马国宏)[1*], Jin Ge (葛 进)[2], Shuhong Hu (胡淑红)[2], and Ning Dai (戴 宁)[2]

[1] *Department of Physics, Shanghai University, Shanghai 200444, China*

[2] *National Laboratory for Infrared Physics, Shanghai Institute of Technical Physics, Chinese Academy of Science, Shanghai 200083, China*

[*] *Corresponding author: ghma@staff.shu.edu.cn*

Received December 13, 2010; accepted January 20, 2011; posted online June 27, 2011

Terahertz (THz) wave transmission through a thin metal film with periodic arrays of subwavelength rectangular holes is investigated systematically. The roles of the waveguide resonances and surface plasmon polaritons (SPPs) in extraordinary transmission are also clarified. The transverse waveguide resonances (hole-shape dependence) dominates the position and width of maximum transmission. In addition, the periodicity of the hole arrays dominates the position of minimum transmission due to the excitation of SPP, which acts as a band-stop filter in the THz transmission spectra. Our results clearly demonstrate that the extraordinary transmission in THz frequency is originated from the transverse waveguide resonances that behave with a SPP-like character. Simulation based on finite-difference time-domain (FDTD) agrees well with the experimental results.

OCIS codes: 040.2235, 240.6680, 230.7370.
doi: 10.3788/COL201109.S10204.

The extraordinary transmission of electromagnetic waves through two-dimensional (2D) arrays of subwavelength holes perforated in thin metallic films has attracted great interest since the pioneering work published by Ebbesen *et al.* in 1998[1]. Subsequently, extensive experimental and theoretical studies have been carried out to elucidate the underlying physics behind the enhanced transmission properties[2,3]. The excitation of coupled surface plasmon polaritons (SPPs) on the upper and lower interfaces of the metal grating[2,4−6] is a widely accepted mechanism for the enhanced transmission. However, Klein *et al.*[7] demonstrated experimentally that extraordinary light transmission was strongly influenced by the individual shape of the hole under study. Using the Fabry-Pérot resonance model, Takakura *et al.*[8] successfully explained the enhancement of the transmission in a thick metallic slit. Through rigorous coupled wave analysis, Cao *et al.* even concluded that the surface plasmons (SPs) played a "negative role" in light transmission through a subwavelength slit array[9]. The theoretical modeling by Ruan *et al.*[10] in a random array of metallic holes demonstrates the importance of the shape resonance in transmission, showing the enhanced transmission results from two different resonances: localized waveguide resonances (i.e., Fabry-Pérot resonance) and SP resonances. However, the exact cause behind the enhanced transmission remains controversial, and there is no global consensus yet. In the terahertz (THz) frequencies, extraordinary transmission phenomena has also caught great attention in recent years[11−15].

In this letter, the transmission properties of the thin metallic film with periodic arrays of rectangular subwavelength holes have been investigated systematically using THz time-domain spectroscopy (THz-TDS) system. A simple but effective analytical model is proposed, which can explain almost all the experimental data including most previous published results successfully. The model reveals that both the shape and periodicity of metallic hole arrays affect the transmission properties of the metallic grating in THz regime, wherein the shapes of metallic hole dominate the position and width of transmission maxima, and the periodicities dominate the position of transmission minima. Our experimental results clearly demonstrate that the extraordinary transmission in THz frequency is caused by the shape resonance of the metallic hole, rather than SPP contribution. Numerical simulation based on finite-difference time-domain (FDTD) agrees well with experimental findings, and the simulational results also show good agreement with experimental data reported in the literature.

Compared with the optical region, THz wave is a very special and interesting part in electromagnetic spectrum. Due to a drastic increase in the value of dielectric function, most metals (such as Al, Ag, Au, and Cu) resemble in many ways a perfect electronic conductor (PEC), and the negligible penetration depth of the electromagnetic fields indicates that a flat metallic film does not support any SPP. However, the designed SPPs (or say spoof-SPPs) occur in a metallic film perforated with periodical hole arrays[16]. The spoof-SPPs play very similar roles as the real ones. Although the energy position of the spoof-SPP is overlapped completely with that of Rayleigh anomaly in the THz region for a PEC film, their contributions to light transmission are distinguished due to the different characteristics of the Rayleigh anomalies and SPPs.

In 1902, Wood discovered that the order of diffraction will vanish when it emerges tangent to the plane of the grating. Later, Rayleigh explained these anomalies under the name "passing-off orders". Therefore, the wavelengths of Rayleigh anomalies can be obtained from the

grating equation for normal incidence as expressed by[17]:

$$\lambda_{\mathrm{R}} = \frac{L}{\sqrt{i^2 + j^2}} n, \tag{1}$$

where n is the wavelength dependent refractive index of surrounding medium, i and j are integers, and L is the lattice constant of grating. The "passing-off orders" are for the first and higher orders, rather than for the zero-order. Therefore, as in most studies, if we focus on the zero-order transmission of light, Rayleigh anomalies, as reported by several previous works[18−20], indicate a "discontinuity" in a transmission spectrum, rather than the transmission minima. Rayleigh anomaly denotes that the energy of evanescent diffracted order is being redistributed among the remained propagating orders (including zero-order), which is the origin of the "discontinuity" in the zero-order diffraction. On the other hand, the wavelength of SPP resonance in a periodical structure for normal incidence is characterized by the dispersion relation:

$$\lambda_{\mathrm{sp}} = \frac{L}{\sqrt{i^2 + j^2}} \sqrt{\frac{\varepsilon_{\mathrm{m}} \varepsilon_{\mathrm{d}}}{\varepsilon_{\mathrm{m}} + \varepsilon_{\mathrm{d}}}}, \tag{2}$$

where λ_{sp} is the vacuum wavelength of the excited SPP; ε_{m} and ε_{d} are dielectric constants of metal and dielectric surrounding, respectively.

As mentioned previously, in THz frequency, the dielectric constant of metal is several orders higher than that of dielectrics, i.e., $\varepsilon_{\mathrm{m}} \gg \varepsilon_{\mathrm{d}}$, and the metallic film can be treated as an ideal metal. Hence, Eqs. (1) and (2) can be unified as:

$$\lambda_{\mathrm{sp}} = \lambda_{\mathrm{R}} = \frac{L\sqrt{\varepsilon_{\mathrm{d}}}}{\sqrt{i^2 + j^2}}. \tag{3}$$

It indicates that the wavelengths of SPP excitation are overlapped completely with those of the Rayleigh anomalies in the THz frequency region.

As for an individual metallic hole, there exists a shape-dependence waveguide mode. Here, we consider a rectangular subwavelength hole as a cavity, the waveguide resonances are composed of two components: transverse and longitudinal modes. The metal film investigated in the present study is a thin metal film with a thickness of about hundreds of nanometers. The wavelengths of our THz wave source are hundreds of micrometers, which are much larger than the cut-off wavelength of longitudinal modes. Therefore the longitudinal modes are not supported in the thin film, and only the transverse waveguide mode is taken into account as the mechanism of localized resonance, which is also called half-wavelength resonance in transverse direction[21,22].

The samples in this study are metal rectangular hole arrays fabricated on fused silica substrate. Briefly, an Al layer with a thickness of about 220 nm was deposited on a fused silica substrate by magnetron sputtering technique, with photolithography processing to form a designed metal rectangular hole arrays. Figure 1 shows the optical image of a typical structure with a period of 200 μm. For THz spectroscopy characterization, a transmission THz-TDS in the frequency range of 0.1−2.0 THz was used. Details of the THz-TDS system are described in our previous papers[23,24]. The waveform of the THz wave in the time domain was measured directly, and the amplitude and phase spectra were obtained by Fourier transform from the time-domain waveforms. A blank fused silica with the same thickness was also used as a reference. The refractive index of fused silica changed little over the investigated frequency, and it was treated as a constant of about 1.95 in this study. This is very close to the value reported in a previous work[25].

The FDTD simulation was based on EASTFDTD software. In our simulations, the incident wave with frequency ranged from 0 to 2.0 THz, propagated along the z-direction and illuminated (at normal incidence) on a metal film drilled with periodic hole arrays on fused silica substrate. The THz waves propagated with polarization perpendicular to the long edge of the rectangular holes. Periodic boundary conditions were applied to the both the x- and y-directions, and a perfectly matched layer (PML) boundary condition was applied in the z-direction. Due to the fact that the thickness of the substrate was much larger than that of the metal film, and thickness of silica substrate was considered as a semi-infinite. In addition, because of a very large negative dielectric constant in the THz frequency (on the order of 10^5∼10^6) for most metals, the conductivity of the AL film is usually taken as perfect conductor during FDTD simulation. For the transmission and reflection spectra calculation, we only collected the data from the zero-order diffraction.

First, we study the role of the hole periodicity in the behavior of the zero-order transmission of the rectangular hole arrays. In order to investigate the role of Wood's anomaly, three samples were designed and had a hole shape of 150×50 (μm) and with varied periodicities of 180, 200 and 220 μm, respectively.

In the measurement, the THz waves with polarization perpendicular to the long edge of the rectangular holes ($\mathbf{E} \perp x$) impinge on the sample at normal incidence (Fig. 1). The THz wave transmission through the arrays was normalized to the substrate of the array in order to obtain the transmission of the holes[1,7,10]. Figure 2 shows the transmission spectra of the samples at normal incidence. It is clearly seen that the positions of transmission minima are localized at 0.7, 0.77, and 0.85 THz for the structures with periodicities of 220, 200 and 180 μm, respectively. According to Eq. (3), such transmission minimum is related to the excitation of (1, 0)-mode SPP at

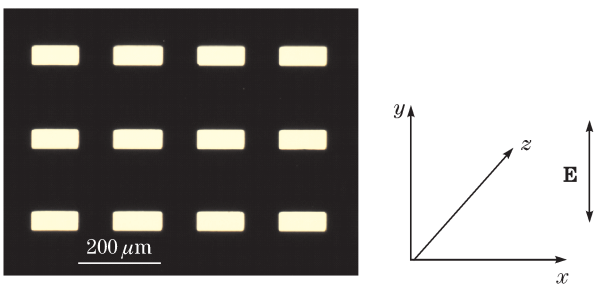

Fig. 1. Optical image of the metallic hole array with a structure of 120 × 50 (μm) and periodicity of 200 μm on fused silica substrate. The structural parameters of all samples have 2% deviation from those of designed structures.

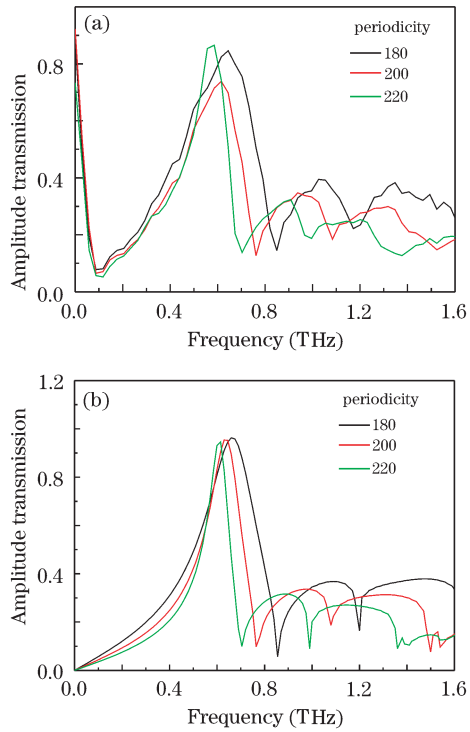

Fig. 2. (a) Measured transmission spectra of the structures 150 × 50 (μm) with periodicities of 180, 200 and 220 μm on fused silica substrate, respectively; (b) Calculated transmission spectra of the structures in (a).

the substrate-metal interface. The resonant frequency of SPP at the air-metal interface is much higher than that at the substrate-metal interface, e.g., the frequency of (1, 0)-mode SPP at Al-air interface is 1.5 THz for the sample with a periodicity of 200 μm. The large SPP frequency difference between air-metal and substrate-metal interfaces hinders the coupling efficiency across the metallic hole, leading to transmission minimum at the SPP frequency. The peak position of the transmission shows a slight redshift (i.e., from 0.63 to 0.58 THz) as the periodicity of the structure increased from 180 to 220 μm. We attribute the transmission maximum to the contribution of half-wavelength resonance from the cut-off waveguide mode (Fig. 2(a)).

The position of transmission minima (or resonant frequency of SPP) shifted to low frequency with an increase in periodicity; as a result, the high frequency side of the waveguide transmission profile was possibly cut off by the periodicity-related transmission minima. Thus, the final transmission profile provides a cheating phenomenon which makes it look like the shift of the transmission peak. In previous works[12−14], the frequencies of the SPP resonance corresponded to the position of transmission minima, rather than transmission maxima. The periodicity independence of transmission peak indicates that the SPP resonance is not the key mechanism responsible for the enhanced transmission in the THz region. Using the FDTD method, numerical simulations were performed on the samples whose geometrical parameters were set to be the same as those in the experiment. The simulation results shown in Fig. 2(b) reveal that they are in good agreement with the experimental results, except for the peak transmission intensities. The simulated results also show slightly higher amplitude transmission due to lossless characteristics of PEC.

In order to recognize the originality of the transmission peak further, another set of samples were designed and fabricated. This time, the period of hole arrays was fixed at d=200 μm, and the shapes of the rectangular holes were set at 50×50, 100×50, 120×50 and 150×50 (μm), respectively. The polarization of the incident wave was kept perpendicular to the long edge of the rectangular holes. The normalized zero-order transmission is shown in Fig. 3(a). It is obvious that the minima of transmission are all located at the same position, 0.77 and 1.08 THz, which originated from (1, 0)-mode and (1, 1)-mode SPP, respectively, at the substrate-metal(S/M) interface (Eq. (3)), as shown in Fig. 3(a). The positions of transmission maxima show hole-shape dependence, and the resonance frequency shifted from 0.61 to 0.72 THz, with the long edge length of the rectangular holes decreasing from 150 to 100 μm. It should be mentioned that we only varied the length of the edge perpendicular to the THz wave polarization, and the length of the other edge as well as the periodicity of the arrays remained same. Thus, it is easy to conclude that it is the localized waveguide resonances, rather than SPP, that led to the transmission enhancement. For the sample consisting of 50×50 (μm) rectangular apertures, because the wavelength of the THz source is larger than the cut-off wavelength of the hole waveguide, the transmission is too low to be detected in our setup. Figure 3(b) shows the calculated transmission spectra of the structures as those measured in the experiment using FDTD simulation. There is a good agreement of the peak position and bandwidth between the experimental results and theoretical simulation.

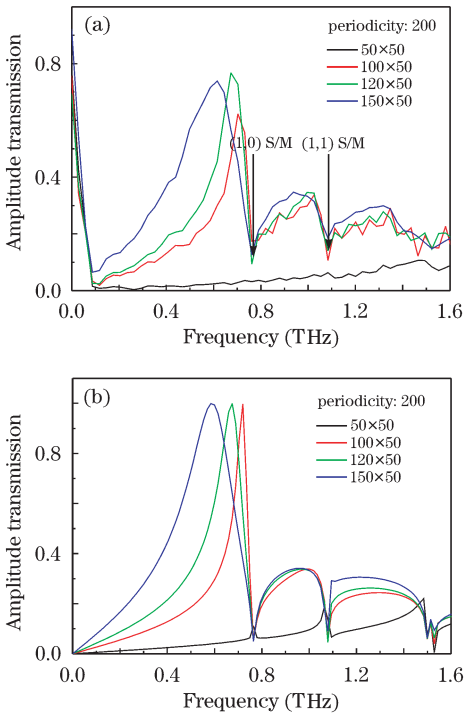

Fig. 3. (a) Measured transmission spectra of the structures 50 × 50, 100 × 50, and 150 × 50 (μm), all with periodicity of 200 μm on fused silica substrate; (b) calculated transmission spectra of the structure in (a).

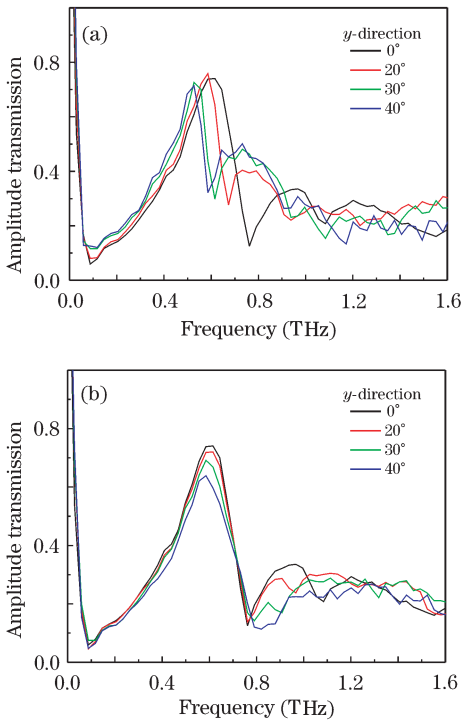

Fig. 4. The transmission spectra of the structure 150 × 50 (μm) with periodicity of 200 μm with different incident angle deviates from the (a) y-axis and (b) x-axis.

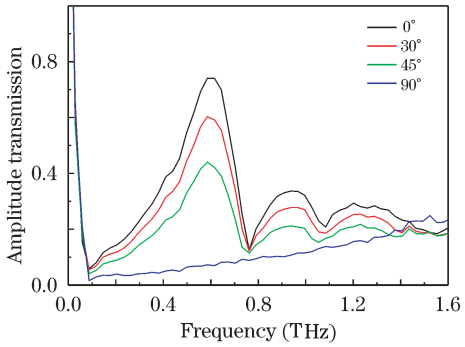

Fig. 5. The transmission spectra of the structure 150×50 (μm) with periodicity of 200 μm when change the polarization of the incident light deviates from the y-axis.

As analyzed above, the transverse localized waveguide resonance led to the extraordinary transmission. Assuming that the lengths of the short and long edge of the rectangular hole are a and b, respectively, the transmission peak at the fundamental shape resonance can be written as $\lambda_{\rm res} = 2n_{\rm eff}b$[21,22], where $n_{\rm eff}$ is the effective index of the fundamental waveguide mode related to the refractive index of air and substrate, the magnitude lies between 1 and $n_{\rm s}$[26]. Here, $n_{\rm s}$ is the refractive index of the substrate.

The waveguide resonance frequency shifts towards the frequency of (1,0)-mode SPP on the substrate-metal interface with the decrease of the length of the long edge of the rectangular hole (Fig. 3). As a result, the transmission peak profile will be strongly affected by spoof-SPP. For transmission measurement, incident light coupled with the spoof-SPP mode of both sides of metal film, but the SPP frequencies on both interfaces did not overlap at all in our case due to the large energy difference. As a result, the excitation of SPP led to loss of light transmission. With this phenomenon, it is reasonable to understand why the most transmission maximum always appears on the lower frequency part of the SPP. In our case, SPP acts as a "band-stop filter" for light transmission, modifying the waveform of the localized waveguide resonance. When the frequencies of waveguide resonance and SPP were close enough, the position of the transmission peak was dominated by both waveguide mode and SPP mode. The transmission peak of the structure of 100×50 (μm) was incomplete, which was "cut" by the "SPP filter."

With referring to the coordinate shown in Fig. 1, light incident angle dependence of THz wave transmission is investigated. In this study, the hole arrays with a size of 150×50 (μm) and periodicity of 200 μm was used.

At first, we changed the incident angles along the y-axis. In the experiment, what we did was to rotate the sample along the x-axis. According to conservation of momentum, the incident light also provided an in-plane momentum for SPP excitation, and Eq. (3) can be rewritten as:

$$\lambda_{\rm sp} = \lambda_{\rm R} = \frac{L}{\sqrt{i^2 + j^2}}(n + \sin\theta), \tag{4}$$

where n is the refractive index of air or substrate. It should be noticed that the wavelengths of SPP excitation are overlapped completely with that of Rayleigh anomalies at all conditions for PEC film; in addition, both of them show same incident angle dependence. By changing the incident angle from 0° (normal incident) to 40°, Figure 4(a) shows angle dependence of the transmission spectra of the structure 150×50 (μm). In addition, the position of (1, 0)-mode SPP on the substrate-metal interface shifted from 0.77 to 0.58 THz, with incident angles varying from 0 to 40 degree, which is in good agreement with the prediction from Eq. (4). The transmission maximum position also showed a negligible shift when the incident angle was smaller than 20°. As the incident angle increased further, the transmission peak seems to have shifted to a lower frequency due to the overlapp effect of the SPP "filter" and waveguide resonance. The incident angle dependence of transmission spectra provides evidence that it is the localized waveguide resonance, and not the SPP resonance, that has led to the enhanced transmission.

Next, we change the incident angles along the x-axis by rotating the sample along the y-axis. This kind of rotation provides an in-plane momentum along the x-direction, which does not affect the (1, 0)-mode SPP and Rayleigh anomaly at the substrate-metal interface. However, with the increase of the rotation angle, the transmitted energy in the z-direction decreases. The decrease of energy in transverse waveguide resonance can weaken the transmission peak; the result is presented in Fig. 4(b).

In the experiment, we changed the polarization of the incident light at normal incidence. The polarization of the THz wave was in the XY plane. When the polarization of the incident light deviated from the y-axis, the component along the x-axis was not zero. For the x-direction polarization, the cut-off frequency was 3 THz,

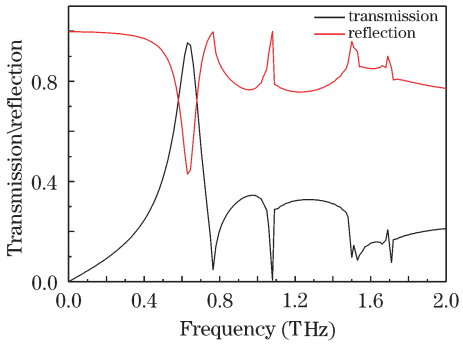

Fig. 6. The simulated transmission and reflection spectra of the structure 150 × 50 (μm) with periodicity of 200 μm at normal incidence.

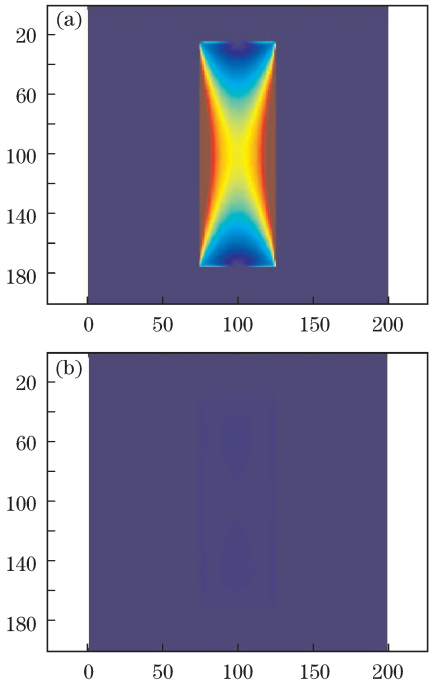

Fig. 7. Calculated electric field distribution for the structure of 150 × 50 (μm) with periodicity of 200 μm under excitation frequencies at (a) 0.61 THz (waveguide mode) and (b) 0.77 THz (SPP frequency).

much higher than the output frequencies of our THz source. Hence, x-polarized modes are non-propagating waves. At the same time, the decreasing component along the y-axis results in decreasing transmission. The transmission amplitude decreases rapidly with the increase of rotation angle (Fig. 5).

For a PEC, the skin depth of electromagnetic field is zero, or say, there is no loss in PEC film. With periodical arrays of holes perforated on the PEC film, light-matter interaction can be depicted by the excitation of a spoof-SPP, whereby the perfect metal interrupted with a periodical array of holes behave as if it is a real metal in visible frequency regime. The transmission minimum shown in Fig. 3 shows that the energy at the spoof-SPP frequency is dissipated in the film, which is unreasonable for the PEC film. In order to clarify this phenomenon, we calculated the transmission and reflection spectrum of the array 150×50 (μm) with the period of 200 μm at normal incident radiation by FDTD simulation (Fig. 6). The peak of reflectance appeared at 0.77 THz, corresponding to transmission minimum (the resonant position of (1, 0)-mode SPP at the substrate-metal interface). During reflection spectra simulation based on FDTD, we only collected the data from zero-order diffraction; Rayleigh anomaly can be ruled out for the contribution to the reflection peak at $\lambda_{sp}(\lambda_R)$ because the passing off order propagates along the metallic grating surface, and has no contribution to the zero-order reflection. Therefore, we believe that the excitation of SPP at the metal-substrate interface enhances reflection, even leads to total reflection, and as a result transmission spectrum shows a minimum. Although the resonant frequency between Rayleigh anomaly and SPP is overlapped completely for the PEC structure, they show different contributions to the zero-order reflection spectrum, so that we can identify the influence on the transmission and reflection spectra.

As mentioned above, transverse waveguide resonance plays a dominant role in the enhanced transmission in THz regime. To understand the physical process leading to the enhanced transmission and mechanisms of the waveguide resonance inside the rectangular holes, we calculated the electric field amplitude distribution inside the hole at resonant frequency of 0.61 THz (waveguide mode) and 0.77 THz (Rayleigh anomaly) for the structure of 150×50 (μm) with periodicity of d=200 μm (Figs. 7(a) and (b), respectively). As the incident light frequency is on-resonant with the waveguide mode located at 0.6 THz, the electric field distribution inside the hole is not homogeneous. It is clear that transverse waveguide resonance is not a conventional waveguide resonance, but a hybrid character: the mode in vertical (x-axis) direction is a typical waveguide mode, but is laterally evanescent and confined on the edge of the hole in the horizontal (y-axis) direction. The transverse waveguide mode behaves with a SPP-like character. However, it is not a propagating SPP, because it is localized inside metallic hole and shows individual hole-shape dependence. Previous studies called this the "cavity surface-plasmon" (CSP) or "waveguide surface-plasmon" (WSP) mode[20,27,28]. Meanwhile, with the excitation at the SPP frequency of 0.77 THz, amplitudes of electromagnetic field distribution inside the hole are very weak; this result is reasonable because almost 100% incident light is reflected out at 0.77 THz, and no light penetrate into the structure.

In conclusion, the role of the waveguide resonance and SPP in extraordinary transmission has been investigated in the THz regime. For thin metal film with periodic arrays of subwavelength rectangular holes on substrate, the physical mechanism of the extraordinary transmission in THz region can be understood as: transverse waveguide resonance is modulated by the excitation of SPP; shape resonance dominats the maxima of the zero-order transmission, and the excitation of SPP related to period of the arrays acts as a "band-stop filter" to shape the profile of the transmission spectrum; SPP also affects the position of transmission peak when the frequency between waveguide resonance and SPP is close enough. We conclude that the enhanced transmission arises from the transverse localized waveguide resonance, but the transverse waveguide modes behave with a SPP-like hybrid character.

This work was supported by the National Natural Science Foundation of China (No. 10774099), the Science and Technology Commission of Shanghai municipal (No. 09530501100), and the Program for Professor of a Special Appointment (Eastern Scholar) at the Shanghai Institutions of Higher Learning. S. H. Hu and N. Dai would like to thank the financial support from the National High Technology Research and Development (No. 2006AA12Z135) and the National Natural Science Foundation of China (Nos. 10334030, 60225004, and 60221502). Part of the work was also supported by the National Laboratory for Infrared Physics, Chinese Academy of Sciences.

References

1. T. W. Ebbesen, H. J. Lezec, H. F. Ghaemi, T. Thio, and P. A. Wolff, Nature **391,** 667 (1998).
2. X. Fang, Z. Li, Y. Long, H. Wei, R. Liu, J. Ma, M. Kamran, H. Zhao, X. Han, B. Zhao, and X. Qiu, Phys. Rev. Lett. **99,** 066805 (2007).
3. G. Xiao, X. Yao, X. Ji, J. Zhou, Z. Bao, and Y. Huang, Chin. Opt. Lett. **6,** 791 (2008).
4. P. Lalanne, J. C. Rodier, and J. P. Hugonin, J. Opt. A: Pure Appl. Opt. **7,** 422 (2005).
5. J. A. Porto, F. J. Garcia-Vidal, and J. B. Pendry, Phys. Rev. Lett. **83,** 2845 (1999).
6. H. F. Ghaemi, T. Thio, D. E. Grupp, T. W. Ebbesen, and H. J. Lezec, Phys. Rev. B **58,** 6779 (1998).
7. K. J. Klein Koerkamp, S. Enoch, F. B. Segerink, N. F. Van Hulst, and L. Kuipers, Phys. Rev. Lett. **92,** 183901 (2004).
8. Y. Takakura, Phys. Rev. Lett. **86,** 5601 (2001).
9. Q. Cao and P. Lalanne, Phys. Rev. Lett. **88,** 057403 (2002).
10. Z. C. Ruan and M. Qiu, Phys. Rev. Lett. **96,** 233901 (2006).
11. J. Saxler, J. G'omez-Rivas, C. Janke, H. P. M. Pellemans, P. H. Bolivar, and H. Kurz, Phys. Rev. B **69,** 155427 (2004).
12. D. Qu, D. Grischkowsky, and W. Zhang, Opt. Lett. **29,** 896 (2004).
13. H. Cao and A. Nahata, Opt. Express **12,** 3664 (2004).
14. J. Han, A. K. Azad, M. Gong, X. Lu, and W. Zhang, Appl. Phys. Lett. **91,** 071122 (2007).
15. W. Zhang, Eur. Phys. J. Appl. Phys. **43,** 1 (2008).
16. J. B. Pendry, L. Martin-Moreno, and F. J. Garcia-vidal, Science **305,** 847 (2004).
17. T. J. Kim, T. Thio, T. W. Ebbesen, D. E. Grupp, and H. J. Lezec, Opt. Lett. **24,** 256 (1999).
18. A. Hessel and A. A. Oliner, Appl. Opt. **4,** 1275 (1965).
19. M. Sarrazin, J. P. Vigneron, and J. M. Vigoureus, Phys. Rev. B **67,** 085415 (2003).
20. C. P. Huang, Q. J. Wang, and Y. Y. Zhu, Phys. Rev. B **75,** 245421 (2007).
21. F. J. Garcia-Vidal, E. Moreno, J. A. Porto, and L. Martin-Moreno, Phys. Rev. Lett. **95,** 103901 (2005).
22. J. W. Lee, M. A. Seo, D. H. Kang, K. S. Khim, S. C. Jeoung, and D. S. Kim, Phys. Rev. Lett. **99,** 137401 (2007).
23. G. Ma, D. Li, H. Ma, J. Shen, C. G Wu, J. Ge, S. Hu, and N. Dai, Appl. Phys. Lett. **93,** 211101 (2008).
24. D. Li, G. Ma, J. Ge. S. Hu, and N. Dai, Appl. Phys. B **94,** 623 (2009).
25. D. Grischkowsky, S. Keiding, M. van Exter, and C. Fattinger, J. Opt. Soc. Am. B, **7,** 2006 (1990).
26. J. H. Kang, J. H. Choe, D. S. Kim, and Q. H. Park, Opt. Express **18,** 15652 (2009).
27. X. Yin, C. Huang, Z. Shen, Q. Wang, and Y. Zhu, Appl. Phys. Lett. **94,** 161904 (2009).
28. J. Gu, Z. Tian, Q. Xing, C. Wang, Y. Li, F. Liu, L. Chai, and C. Wang, Chin. Opt. Lett. **8,** 1057 (2010).